Comparative Study of Electro-pneumatic Actuator Performance Using Linear, Sliding Mode and Hybrid Position Control Laws

SHAWKI Al-SALOUM, ALI TAHA, IBRAHIM CHOUAIB
Department of electronic and mechanical systems
Higher Institute for Applied Sciences and Technology (HIAST)
Damascus
SYRIA
shawki.alsaloum@hiast.edu.sy, alitaha1267@gmail.com, ibrahim.chouaib@hiast.edu.sy

Abstract: - This paper presents a comparative study of linear, sliding mode and hybrid control laws for an electro-pneumatic actuator in the context of position control. The linear controllers include gain-scheduled-proportional-velocity-acceleration and proportional-derivative. The sliding mode controllers include first, second and third order sliding mode control laws. The hybrid controllers are combinations of linear and sliding mode control laws. More precisely, two hybrid controllers have been designed, the first uses gain-scheduled-proportional-velocity-acceleration control law as sliding variable for the first order sliding mode controller, and the second considers the proportional-derivative control law as sliding variable for the second order sliding mode controller. The experimental results showed that the hybrid control laws improve the robustness of the first and second order sliding mode control; also they improve time and frequency response characteristics of the closed-loop. The analysis of experimental results showed the performance of each control law. The main conclusion of results analysis is that the third order sliding mode control law realizes better bandwidth and the second hybrid control law realizes better settling time under load and better position accuracy besides the good bandwidth and the ease of implementation.

Key-Words: - Linear control law, sliding mode control, sliding variable, electro-pneumatic actuator.

1 Introduction

Electro-pneumatic servo actuators are commonly used in various applications, especially in positioning, because they have many advantages like low cost, lightness, durability and cleanness when compared with the hydraulic actuators. On the other hand, pneumatic actuators have some undesirable characteristics which derive from the high compressibility of the air, parameters uncertainties, load disturbances, and from the nonlinearities presence in pneumatic systems.

The main control approach which deals with model uncertainties and disturbances is the robust control. The sliding mode control is a nonlinear robust control technique which can compensate the nonlinear behavior of the electro-pneumatic actuator, and it has now become a common control method for the electro-pneumatic actuators due to the advantage of low sensitivity to plant parameter variations and disturbances, which eliminate the necessity of exact modeling.

Sliding mode control is based on the concept of changing the controller's structure, with reference to the motion of the states of the system along predefined manifold, in order to obtain the desired response. In sliding mode, system is governed by the sliding surface [1]. The first step of sliding mode control design is to select a sliding variable which models the desired closed-loop performance in state space.

The design of linear control laws is relatively easy because there are systematic design ways for them. So, the hybrid control law idea is summarized as follows: the linear control law that has relative degree one with respect to the control input can be chosen as a sliding variable of first order sliding mode controller, and the linear control law that has relative degree two with respect to the control input can be chosen as a sliding variable of second order sliding mode controller. Where, the relative degree is defined as the order of the derivative of the sliding variable, in which the control input appears explicitly. Thus, in the case of electro-pneumatic actuator, the linear controller: gain-scheduled-proportional-velocity-acceleration (GSPVA) serves as sliding variable for first order sliding mode controller, and the linear controller: proportional-derivative (PD) serves as sliding variable for second

order sliding mode controller as will be seen later in this paper.

The electro-pneumatic positioning systems have been studied in literature. In [2], adaptive controllers have been designed and implemented in a manipulator robot, driven by electro-pneumatic systems. In [3], a back-stepping based control law is synthesized to take advantage of the system two degrees of freedom and a through tuning method of the closed-loop stiffness and damping is provided. In [4], a state feedback nonlinear controller was proposed for a pneumatic cylinder by using the theory of homogeneous, finite time stable, ordinary differential equations. In [5], a comparison between two positioning linear control laws (a fixed gains control law and a control law with scheduling gains) of an electro-pneumatic asymmetrical cylinder is made in point to point displacement aim. In [6], [7], [8] and [9], sliding mode controller have been designed to ensure position tracking with high precision.

In the second section of this paper, the nonlinear and linear model of the electro-pneumatic actuator will be presented. In the third section, the specifications of the electro-pneumatic system under interest will be detailed. In the fourth section, the linear controllers: gain-scheduled-proportional velocity-acceleration (GSPVA) and the proportional-derivative (PD) will be designed and implemented. In the fifth section, the first order sliding mode controller (FOSMC), the second order sliding mode controller represented by supper twist algorithm (STA) and the third order sliding mode controller (TOSM) will be designed and implemented. In the sixth section, the hybrid controllers will be implemented after clarifying their theoretical principle. The analysis of results and the performance of each controller for the electro-pneumatic actuator will be presented in the seventh section.

2 The Electro-pneumatic Actuator Model

Following standard assumptions on the pneumatic part of the electro-pneumatic system in [6], [5] and [8], as the dynamics of the servo valve is neglected, assuming that the dry friction forces which act on the moving part and the external force acts on the piston rod are considered as disturbances, a nonlinear model for the whole electro-pneumatic as single input system reads as:

$$\begin{cases} \dfrac{dy}{dt} = v \\[2mm] \dfrac{dv}{dt} = \dfrac{1}{M}\left(S(p_1 - p_2) - bv\right) \\[2mm] \dfrac{dp_1}{dt} = \dfrac{krT}{V_1(y)}\left(q_1(u, p_1) - \dfrac{S}{rT}p_1 v\right) \\[2mm] \dfrac{dp_2}{dt} = \dfrac{krT}{V_2(y)}\left(q_2(-u, p_2) + \dfrac{S}{rT}p_2 v\right) \end{cases} \quad (1)$$

With y the piston position, $v = \dot{y}$ its velocity, p_1 and p_2 the pressures of cylinder chambers 1 and 2, $V_1(y)$ and $V_2(y)$ the volumes of cylinder chambers 1 and 2, S is cylinder cross section area, M is mass of piston and its accessories, T is air source temperature, and k is poly-tropic index. There is uncertainty in the values of the parameters: k, T, φ, ψ and b. The model of mass flow rate delivered by the servo distributor can be reduced to a static function described by two relationships $q_1(u, p_1)$ and $q_2(-u, p_2)$. The term (bv) represents viscous friction where b is viscosity factor, the external force due to atmospheric pressure is neglected. In order to get an affine nonlinear state model, the mass flow rate static characteristic issued from measurements is written as a function of control input u and polynomial functions of p_1 and p_2 as in [5] yields:

$$\begin{cases} q_1(u, p_1) = \varphi(p_1) + \psi(p_1, sgn(u))u \\ q_2(-u, p_2) = \varphi(p_2) - \psi(p_2, sgn(-u))u \end{cases} \quad (2)$$

Where, $\varphi(p_1)$ and $\psi(p_1, sgn(u))$ (resp. $\varphi(p_2)$ and $\psi(p_2, sgn(-u))$) are fifth order polynomial functions with respect to p_1 (resp. p_2). Thus, the system (1) can be rewritten as a single-input uncertain nonlinear system as follows:

$$\begin{cases} \dot{x} = f(x) + g(x)u \\ y = h(x) \end{cases} \quad (3)$$

Where $x = [\, p_1, p_2, v, y\,]^T \in \mathbb{R}^4$ is the state vector, $u \in \mathbb{R}$ the control input, $y \in \mathbb{R}$ the measured smooth output, and $f, g \in \mathbb{R}^4$ are uncertain smooth nonlinear functions.

By using the first order development of the Taylor's series around the equilibrium point $(p_1^e = p_2^e,\ u^e = 0)$ in any position $y = y^e$ [8], and then by combining the state equations associated with the pressures, the acceleration's dynamics can be deduced and the reduced linear model of position, velocity and acceleration can be obtained as in [5], [8] and [10]:

$$\frac{d}{dt}\begin{bmatrix} y \\ \dot{y} \\ \ddot{y} \end{bmatrix} = \begin{bmatrix} 0 & 1 & 0 \\ 0 & 0 & 1 \\ 0 & -\omega_{ol}^2(y) & -2\xi_{ol}(y)\omega_{ol}(y) \end{bmatrix} \begin{bmatrix} y \\ \dot{y} \\ \ddot{y} \end{bmatrix}$$
$$+ \begin{bmatrix} 0 \\ 0 \\ \Psi_{ol}(y) \end{bmatrix} u \qquad (4)$$

Thus, the third-order transfer function $A(P)$ of the electro-pneumatic actuator in the equilibrium in any position $y^e = y$ is obtained as follows:

$$A(P) = \frac{Y(P)}{U(P)}$$
$$= \frac{\Psi_{ol}(y)}{P(P^2 + 2\xi_{ol}(y)\omega_{ol}(y)P + \omega_{ol}^2(y))} [m/V] \quad (5)$$

Where $\Psi_{ol}(y)$ the gain, $\omega_{ol}(y)$ the pulsation and $\xi_{ol}(y)$ the damping ratio are functions of piston position as is depicted in figure (3) with calculation step $1\,[mm]$ and P is the Laplace-domain variable.

3 The Specifications of the Electro-pneumatic System

The electro-pneumatic system under interest (in-house developed) is a double acting actuator controlled by a jet pipe servo valve (see Figure (1)) and composed of two chambers denoted 1 and 2. The piston diameter is 84 [mm] and rod diameter is 12 $[mm]$. The pressure source is $p_s = 10\,[bar]$ and the maximum actuator force is 5000 $[N]$. The air mass flow rates q entering the chamber are modulated by single-stage open loop jet pipe servo valve controlled by microcontroller. The pneumatic jack horizontally moves the piston and its accessories of mass M. The piston rod is coupled to a spring (maximum load) which restrains the displacement of the piston and its accessories and restores the initial position in the middle of the total stroke that is equal to $50\,[mm]$ for a total of $80000\,[N/m]$ rate. A dry friction is added to the piston rod with a maximum value is equal to 20 $[N]$. The position sensor is the potentiometer integrated with the piston rod with accuracy of 0.03% FS. The force sensors range is 500 $[Kgf]$ and its non-linear error is less than 0.03% FS. The pressure sensor range is 10 [bar], the accuracy is 0.05% FS, and 1 [KHz] bandwidth. Pressure source temperature is measured with an exposed type K thermocouple with accuracy 1°[K]. All measurements of input and output signals have been made in real time by the rapid prototyping board (Model 626-Sensoray) with

sampling time $t_s = 1\,[ms]$. Velocity is obtained from position signal derivation via the real differentiator with low-pass filter [11] depicted in figure (2), which it has been modified to be suitable for sampling time $t_s = 1\,[ms]$. Then the the direct numerical derivation of the velocity signal gives the acceleration signal. Let X denotes the physical domain defined as:

$$X = \{x \in \mathbb{R}^4, 1\,[bar] \leq p_1, p_2 \leq 10\,[bar],$$
$$-25\,[mm] \leq y \leq +25\,[mm],$$
$$v \leq 0.2\,[m/s]\}$$

And U denotes the control input defined as:
$U = \{u \in \mathbb{R}, |u| \leq 1.5\,[V]\}$.
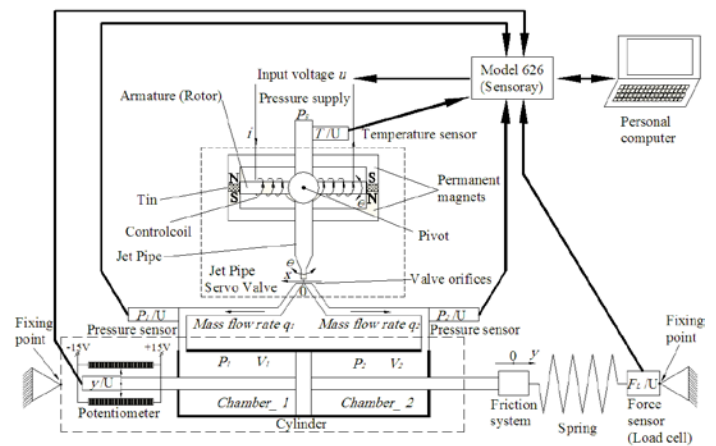
Fig. 1- Electro-pneumatic system scheme.
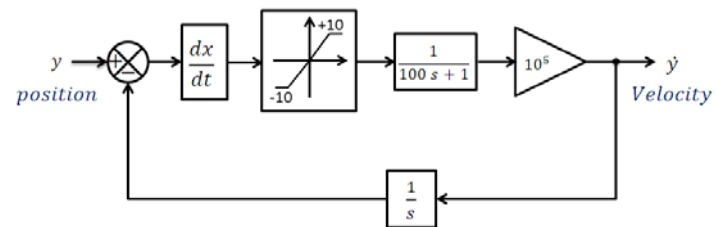
Fig. 2- The real differentiator with low-pass filter in control loop.

4 Linear control laws

4.1 Gain-Scheduled-Proportional-Velocity-Acceleration Controller (GSPVA)

The proportional-velocity-acceleration (PVA) controller is a classic controller, which has features that make it attractive for tracking applications, because it does not only reacts to the present error, but also reacts to the future error by the velocity and acceleration terms.
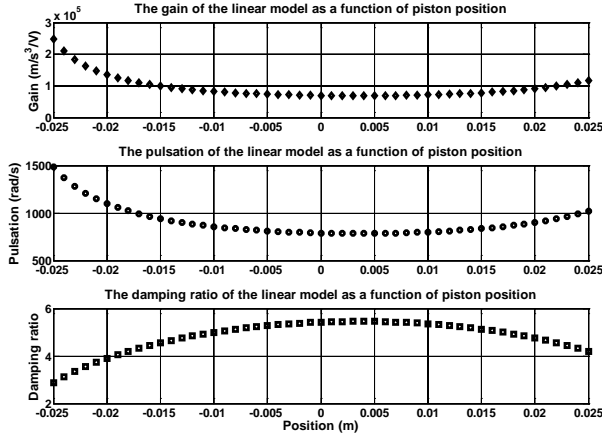
Fig. 3- The evolution of the linear model characteristics as function of position

The design of this controller is based on linear model of the electro-pneumatic actuator described in equation (4).

The linear control law: proportional-velocity-acceleration (PVA) is given as follows:

$$u = -[K_p K_v K_a][e \; v \; a]^T \tag{6}$$

With K_p proportional gain, K_v velocity gain, K_a acceleration gain, $e = y - y_d$ position error, $v = \dot{y}$ piston velocity, $a = \ddot{y}$ piston acceleration and y_d desired position.

The strategy is to impose a closed loop pole placement according to a desired polynomial of the third order for the closed loop system as follows [5]:

$$(P^2 + 2\omega_{cl}\xi_{cl}P + \omega_{cl}{}^2)\left(P + \frac{1}{\tau_{cl}}\right) \tag{7}$$

With the following choices:

- The damping coefficient of the closed loop is chosen as $\xi_{cl} = 0.7071$, because this value achieves good response speed with an appropriate overshooting.
- The pulsation of the closed loop is chosen as $\omega_{cl} = 0.4\,\omega_{ol}$, because this value gave good experimental results.
- The pulsation $1/\tau_{cl}$ is chosen as $1/\tau_{cl} = 6\omega_{cl} = 2.4\,\omega_{ol}$ because this choice gives good bandwidth and good noise rejection.

The state feedback gains are calculated via Ackermann's formula in a linearization point and are given as follows:

$$\begin{cases} K_p = \dfrac{6\omega_{cl}^3}{\Psi} = \dfrac{0.384\omega_{ol}^3}{\Psi} \\[2mm] K_v = \dfrac{(1 + 12\xi_{cl})\omega_{cl}^2 - \omega_{ol}^2}{\Psi} \\[2mm] \quad = \dfrac{0.517632\omega_{ol}^2}{\Psi} \\[2mm] K_a = \dfrac{(6 + 2\xi_{cl})\omega_{cl} - 2\omega_{ol}\xi_{ol}}{\Psi} \\[2mm] \quad = \dfrac{(2.96568 - 2\xi_{ol})\omega_{ol}}{\Psi} \end{cases} \tag{8}$$

Then the calculation is repeated at various linearization points (on whole stroke with calculation step 1 [mm]) to obtain a mapping of the gains depending on the position of the actuator piston. The analytical values of the state feedback gains are given in the equation (9) and depicted in the figure (4).

$$\begin{cases} K_p(y) = 3.795 \times 10^{12}\,y^6 - 7.177 \times 10^{10}\,y^5 \\ \quad -6.663 \times 10^8\,y^4 + 1.214 \times 10^7\,y^3 + \\ 1.474 \times 10^6\,y^2 - 1.057 \times 10^4\,y + 2702\,[m/V] \\ K_v(y) = 4.619 \qquad\qquad [m/s/V] \\ K_a(y) = -6540\,y^4 + 95.32\,y^3 + 95.66\,y^2 \\ \quad -0.6765\,y - 0.08928 \qquad [m/s^2/V] \end{cases} \tag{9}$$

The block diagram of the closed loop with (GSPVA) controller is shown in figure (5). The control law was implemented on the rapid prototyping board (Model 626-Sensoray). The real step responses of the closed loop in case of no load and maximum load are shown in figure (6). The real frequency responses of the closed loop with various amplitudes in case of no load and maximum load are shown in figures (7) and (8), respectively.
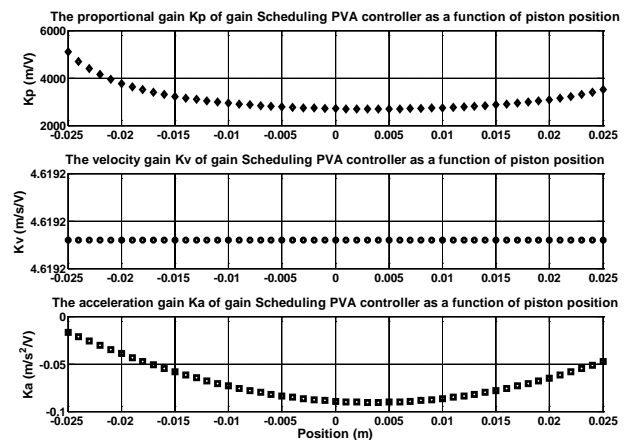
Fig. 4- The evolution of the state feedback gains as function of position.
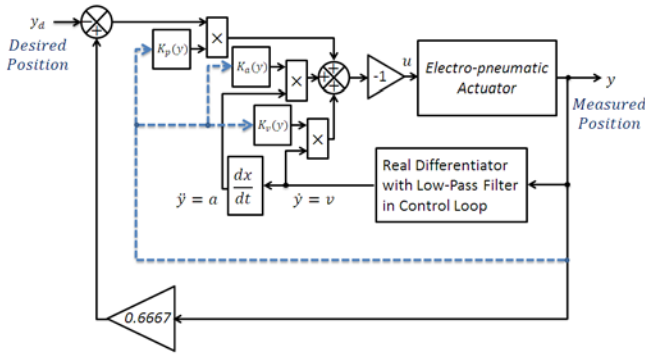
Fig. 5- The block diagram of the closed loop with (GSPVA) controller.
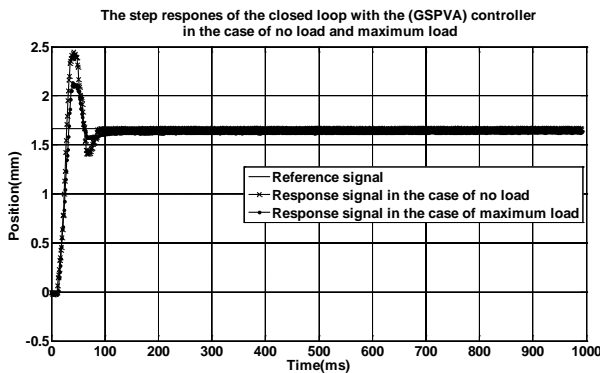
Fig. 6- The step response of the closed loop with (GSPVA) controller in the case of no load and maximum load.
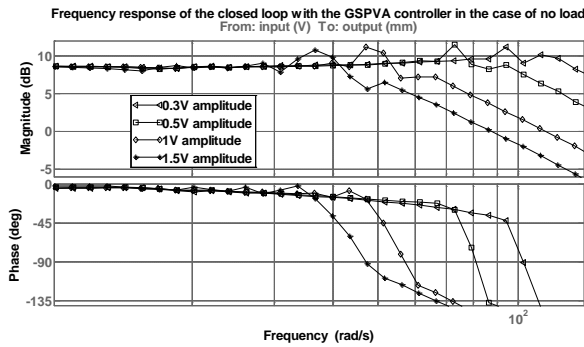
Fig. 7- The frequency response of the closed loop with (GSPVA) controller in the case of no load.
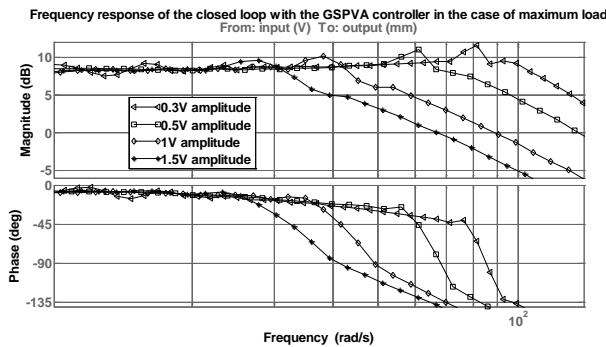
Fig. 8- The frequency response of the closed loop with (GSPVA) controller in the case of maximum load.

4.2 Proportional-Derivative Controller (PD)

The PD controller for the electro-pneumatic actuator has been designed by the second method of (Ziegler-Nichols) [12], where the maximum (or critical) gain was $K_u = 12.5$ and the period of oscillation at the critical gain was $P_u = 0.36 \, [s]$. Thus, the proportional gain is $K_p = 0.6 K_u = 7.5$ and the derivative gain is $K_d = 0.125 P_u = 0.045$. Thus, the PD control law is given as follows:

$$u = K_p \, e + K_d \, \dot{e} = 7.5 \, e + 0.045 \, \dot{e} \qquad (10)$$

Where $e = y_d - y$ is position error, $\dot{e}$ is the direct numerical derivation of the error e . The block diagram of the closed loop with (PD) controller is shown in figure (9). The real step responses of the closed loop in case of no load and maximum load are shown in figure (10). The real frequency responses of the closed loop with various amplitudes in case of no load and maximum load are shown in figures (11) and (12), respectively.
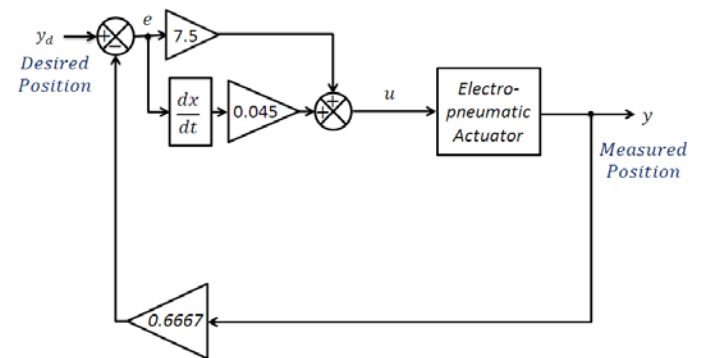
Fig. 9- The block diagram of the closed loop with (PD) controller.
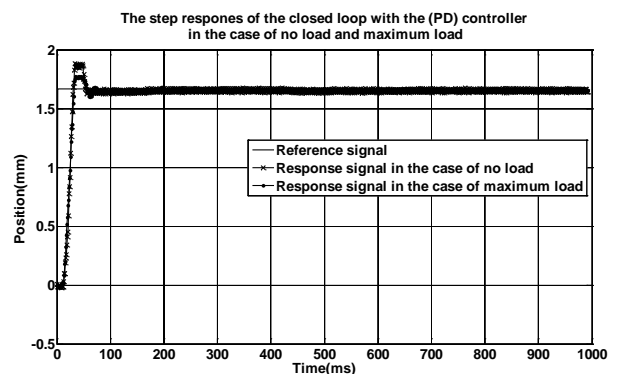
Fig. 10- The step response of the closed loop with (PD) controller in the case of no load and maximum load.
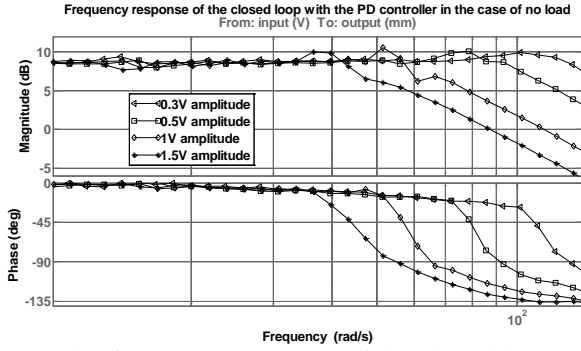
Fig. 11- The frequency response of the closed loop with (PD) controller in the case of no load.
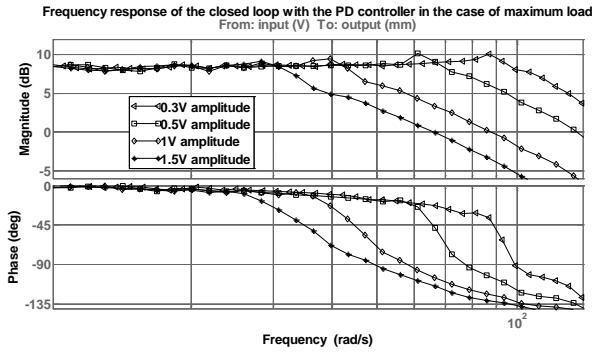
Fig. 12- The frequency response of the closed loop with (PD) controller in the case of maximum load.

5   The Sliding Mode Control Laws

5.1 The First Order Sliding Mode Controller (FOSMC)

The first order sliding mode may be implemented only if the relative degree of the sliding variable s is one with respect to the control input. In the first order sliding mode control, the control acts on the first derivative of the sliding variable $\dot{s}$ to keep the system trajectories in the sliding set ($s = 0$). Hence, $\dot{s}$ is discontinuous in the first order sliding mode control. Therefore, first order sliding mode control is associated with a high frequency switching of the control or chattering. Taking into account the single-input dynamic system (4), where the scalar y is the position of the electro-pneumatic actuator, the scalar u is the control input, and $x = [y, \dot{y}, \ddot{y}]^T \in \mathbb{R}^3$ is the state vector. The control problem is to get the state x to track a specific time varying state $x_d = [y_d, \dot{y}_d, \ddot{y}_d]^T \in \mathbb{R}^3$ in the presence of model imprecision and disturbances. Let $\tilde{x} = x - x_d$ be the tracking error in the variable x. Furthermore, the sliding variable s which is time-varying surface in the state-space $\mathbb{R}^3$ is defined by the scalar equation as follows [13]:

$$s(x,t) = C^T \tilde{x} = [c_1 c_2 \; 1] \begin{bmatrix} y - y_d \\ \dot{y} - \dot{y}_d \\ \ddot{y} - \ddot{y}_d \end{bmatrix}$$

$$= [c_1 c_2 \; 1] \begin{bmatrix} y - y_d \\ \dot{y} \\ \ddot{y} \end{bmatrix} \tag{11}$$

Where c_1 and c_2 are strictly positive constants.

By solving the equation $\dot{s} = 0$ formally for the control input, we obtain an expression for u called the equivalent control u_{eq} which can be interpreted as the continuous control law that would maintain $\dot{s} = 0$ if the dynamics were exactly known [10].

$$u_{eq} = -\left(\frac{c_1 - \omega_{ol}^2(y)}{\Psi_{ol}(y)} \right) \dot{y}$$
$$- \left(\frac{c_2 - 2\omega_{ol}(y)\xi_{ol}(y)}{\Psi_{ol}(y)} \right) \ddot{y} \tag{12}$$

If the equivalent control is chosen equal to zero, yields:

$$\begin{cases} c_1 = \omega_{ol}^2(y) & [1/s^2] \\ c_2 = 2\omega_{ol}(y)\xi_{ol}(y) & [1/s] \end{cases} \tag{13}$$

Thus, the first order sliding mode controller will be a pure discontinues term across the surface $s = 0$.

$$u = -K \, sign(s) \tag{14}$$

Where K is a strictly positive number, it is the maximum voltage which is sent to the electro-pneumatic servo valve ($K = 1.5 \, V$ in this work).

The sliding variable s is previously given in equation (11) and its parameters c_1 and c_2 are given in equations (13) yields:

$$u = -1.5 \, sign(\omega_{ol}^2(y)(y - y_d)$$
$$+ 2\omega_{ol}(y)\xi_{ol}(y)\dot{y} + \ddot{y}) \tag{15}$$

$\omega_{ol}(y)$ and $\xi_{ol}(y)$ are functions of position y as was shown in figure (3). Thus, they can be fitted by two polynomial functions as follows:

$$\begin{cases} \omega_{ol}(y) = 1.107 \times 10^{12} \, y^6 - 2.094 \times 10^{10} \, y^5 \\ \quad -1.944 \times 10^8 \, y^4 + 3.542 \times 10^6 \, y^3 \\ \quad +4.299 \times 10^5 \, y^2 - 3082 \, y \\ \quad +788.3 \qquad\qquad [rad/s] \\ \xi_{ol}(y) = -1.056 \times 10^6 \, y^4 + 1.54 \times 10^4 \, y^3 \\ \quad -2336 \, y^2 + 15.81 \, y + 5.426 \end{cases} \tag{16}$$

The control law was implemented on the rapid prototyping board (Model 626-Sensoray). The

chattering was observed as the high frequency switching which can excite high frequency dynamics neglected in modeling. In general, chattering must be eliminated for the controller to perform properly. This can be achieved by smoothing out the control discontinuity in a boundary layer $\emptyset$ neighboring the sliding surface [13]. Thus, the saturation function can replace the sign function with the boundary layer that achieves good performance for control system. For the electro-pneumatic actuator under interest, the minimum suitable boundary layer is found to be $\emptyset = 400 \ [m/s^2]$ and the first order sliding control law is given as follows:

$$\begin{aligned} u &= -1.5 \ sat(s/\emptyset) \\ &= -1.5 \ sat((\omega_{ol}^2(y)(y - y_d) \\ &\quad + 2\omega_{ol}(y)\xi_{ol}(y)\dot{y} + \ddot{y})/400) \end{aligned} \quad (17)$$

The block diagram of the closed loop with (FOSMC) controller is shown in figure (13). The real step responses of the closed loop in case of no load and maximum load are shown in figure (14). The real frequency responses of the closed loop with various amplitudes in case of no load and maximum load are shown in figures (15) and (16), respectively.
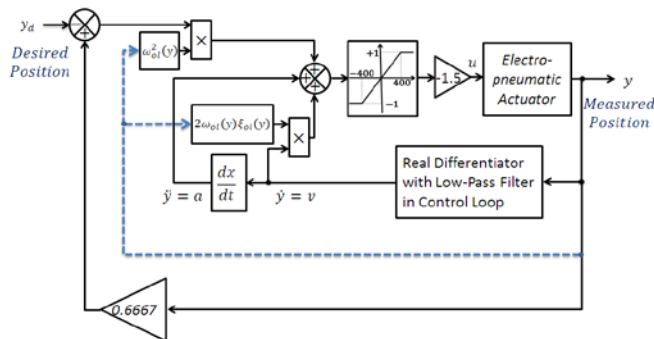
Fig. 13- The block diagram of the closed loop with (FOSMC) controller.
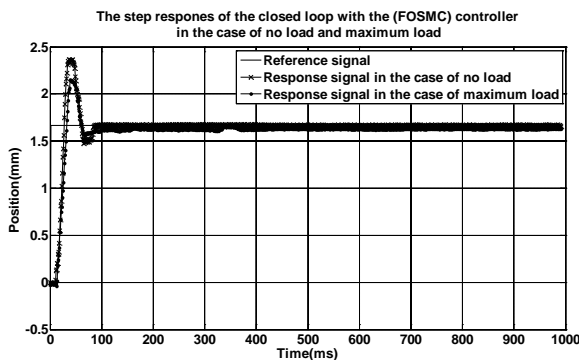
Fig. 14- The step response of the closed loop with (FOSMC) controller in the case of no load and maximum load.
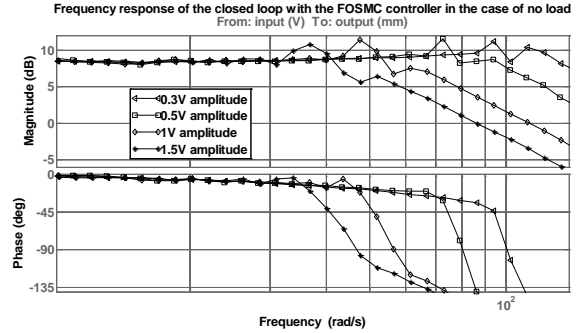
Fig. 15- The frequency response of the closed loop with (FOSMC) controller in the case of no load.
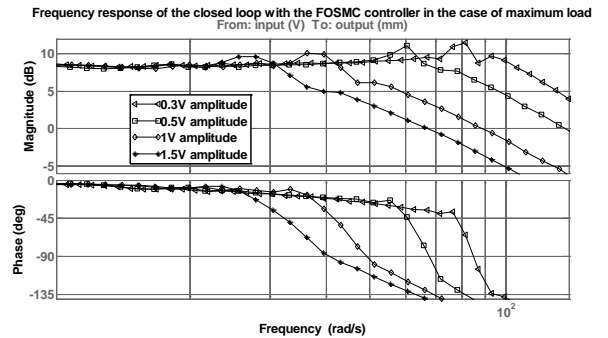
Fig. 16- The frequency response of the closed loop with (FOSMC) controller in the case of maximum load.

5.2 The Second Order Sliding Mode Controller (Super Twist Algorithm (STA))

The super twist algorithm **(**STA) is one of the second order sliding mode control methods. The second order sliding mode control is a special case of the high order sliding mode control and it is called dynamic sliding mode in some references. In the second order sliding mode control, the control acts on the second order time derivative of the sliding variable, instead of influencing the first time derivative as happens in first order sliding mode control. By moving the switching to the higher derivative, chattering is totally eliminated as shown in figure (17).
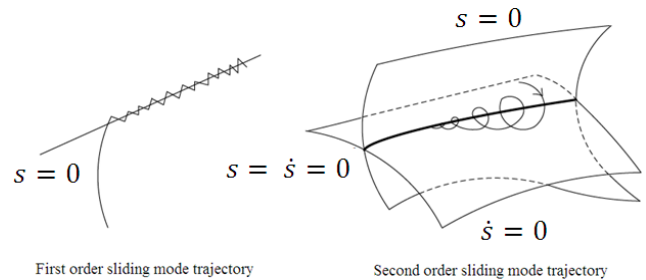
Fig. 17- First and second order sliding mode trajectories.

Consider the single-input nonlinear system defined in (3), let $e = y_d - y$ denote the position error. The sliding variable is defined as follows ([6] and [7]):

$$s = \dot{e} + ce \quad , \quad c > 0 \tag{18}$$

From (1) and (2), the sliding variable relative degree is two. So the second order sliding mode control method (STA) can be implemented. The relative degree equals to two, this means that:

$$\ddot{s} = X(x) + \Gamma(x)u \tag{19}$$

Where X, Γ are real uncertain nonlinear bounded functions, and there are strictly positive constants K_m, K_M, and a positive constant C_0 where $0 < K_m < \Gamma(x) < K_M$ and $|X(x)| \le C_0$.
The objective of (STA) is to ensure the convergence of s and $\dot{s}$ to zero in finite time and to keep them exactly in spite of uncertainties and disturbances.

The simplified form of the super twist algorithm (STA) is as follows [14]:

$$\begin{aligned} u &= -\lambda \ |s|^\rho \ sign(s) + u_1 \\ \dot{u}_1 &= -w \ sign(s) \end{aligned} \tag{20}$$

Where, w, λ, and ρ are positive constant.
The sufficient condition of second order sliding mode surface convergence within limited time is:

$$\begin{cases} w > \dfrac{C_0}{K_m} \\ \lambda^2 > \dfrac{4C_0}{K_m^2} \dfrac{K_M(w + C_0)}{K_m(w - C_0)} \\ 0 < \rho \le 0.5 \end{cases} \tag{21}$$

Moreover, if $\rho = 1$, super twisting algorithm is convergent to origin exponentially [14]. So, the super-twisting control (22) is continuous since the term $\lambda \ |s| \ sign(s)$ is continuous and the term $\int w \ sgn(s)$ is continuous because the high-frequency switching term $sgn(s)$ is "hidden" under the integral [15]. Suppose that in the presence of the bounded disturbance Φ, there is positive constant C where $|\dot{\Phi}| \le C$. Finally, the control law of (STA) is given as follows [15]:

$$\begin{aligned} u &= -\lambda \ |s| \ sign(s) + u_1 \\ \dot{u}_1 &= -w \ sign(s) \end{aligned} \tag{22}$$

Where $\lambda = 1.5\sqrt{C}$, $w = 1.1C$. The control law was implemented on the rapid prototyping board (Model

626-Sensoray). The constant C has been chosen small in the beginning, then it has been increased enough to achieve good performance. In the electro-pneumatic actuator control system the appropriate values of (STA) parameters were: $C = 0.003 \ [V/s]$, and $c = 167 \ [1/s]$.

The block diagram of the closed loop with (STA) controller is shown in figure (18). The real step responses of the closed loop in case of no load and maximum load are shown in figure (19). The real frequency responses of the closed loop with various amplitudes in case of no load and maximum load are shown in figures (20) and (21), respectively.
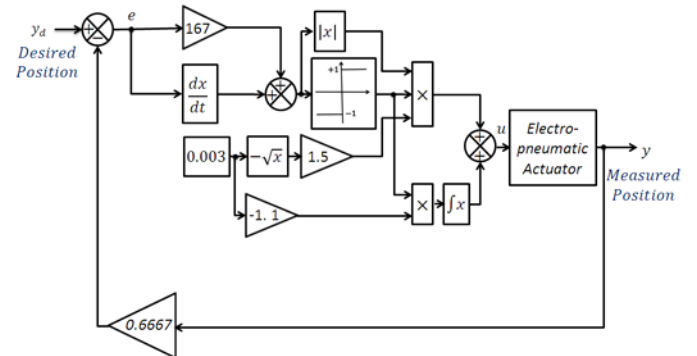
Fig. 18- The block diagram of the closed loop with (STA) controller
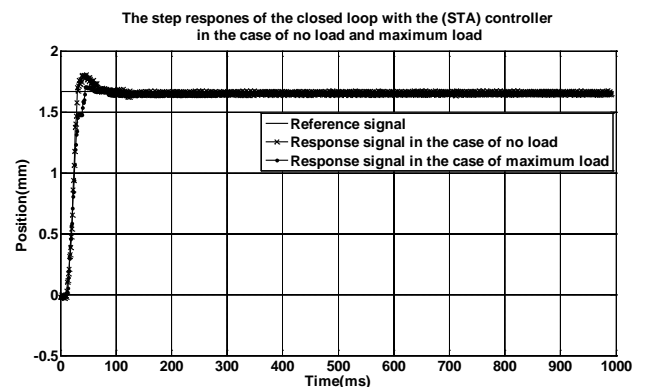
Fig. 19- The step response of the closed loop with (STA) controller in the case of no load and maximum load.
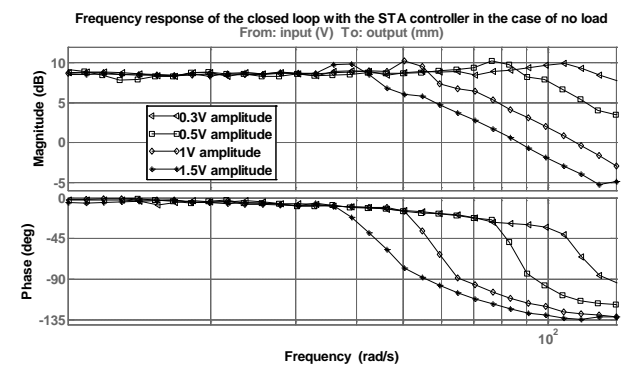
Fig. 20- The frequency response of the closed loop with (STA) controller in the case of no load.
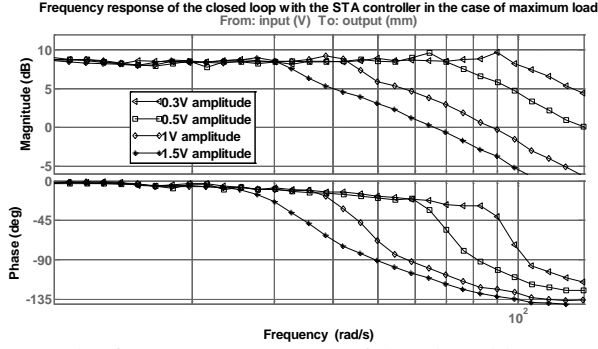
Fig. 21- The frequency response of the closed loop with (STA) controller in the case of maximum load.

5.3 Third Order Sliding Mode Controller with Pre-calculated Trajectories (TOSM)

The control law in this section is based on the tracking of a pre-calculated trajectory which allows the convergence in a known finite time t_F. The main advantages of this control law are [8]:

1. The convergence time is known in advance and the setting of the control law is independent of that time.
2. The sliding mode is established at the initial time, ensuring the robustness of the control law throughout the system response.

The third order sliding mode controller with pre-calculated trajectories (TOSM) is based on a simple idea, the choice of the sliding variable s such that, the system is evolving early from the $t = 0$ on the sliding surface.

In the case of the electro-pneumatic, define the sliding variable s as $s = y - y_d$. From (1) and (2), its relative degree with respect to u equals three which implies that the third order sliding mode controller can be designed. One has:

$$s^{(3)} = X(x) + \Gamma(x)u \qquad (23)$$

Where

$$
\begin{cases}
X(.) = M^{-1}krTS\left(\dfrac{\varphi(p_1)}{V_1(y)} - \dfrac{\varphi(p_2)}{V_2(y)}\right) \\
\qquad -M^{-1}kS^2v\left(\dfrac{p_1}{V_1(y)} - \dfrac{p_2}{V_2(y)}\right) \\
\qquad -(M^{-1})^2b(S(p_1 - p_2) - bv) - y_d^{(3)} \quad (24) \\
\Gamma(.) = M^{-1}krTS\Big(\dfrac{\psi(p_1, sgn(u))}{V_1(y)} \\
\qquad +\dfrac{\psi(p_2, sgn(-u))}{V_2(y)}\Big)
\end{cases}
$$

The control law is defined as [9]: $u = \Gamma_{nom}^{-1}(-X_{nom} + w)$, with Γ_{nom} (respectively X_{nom}) being the nominal value of Γ (respectively X), i.e., derived from (24) with no uncertainty in the values of parameters: k, T, φ, ψ and b, and they are taken to be equal to their nominal values.

The design follows two steps [9]. The first one is constructing the suitable switching variable. The second step is the synthesis of discontinuous control which ensures the convergence in spite of uncertainties/disturbances.

Switching Variable: The switching variable S reads as [9]:

$$
S = \begin{cases}
\dddot{s}(x,t) - \dddot{\mathcal{F}}(t) + 2\xi\omega_n\big[\dot{s}(x,t) - \dot{\mathcal{F}}(t)\big] \\
\qquad +\omega_n^2[s(x,t) - \mathcal{F}(t)] \\
\qquad\qquad\qquad for\ 0 \le t \le t_F \quad (25) \\
\ddot{s}(x,t) + 2\xi\omega_n\dot{s}(x,t) + \omega_n^2 s(x,t) \\
\qquad\qquad\qquad for\ t > t_F
\end{cases}
$$

Where $\mathcal{F}(t) = Ke^{Ft}\mathcal{T}s(0)$ is calculated online and K is calculated offline [9] and its value is shown in figure (22). $\xi = 4$ and $\omega_n = 632\ rad/s$ (ω_n has been chosen close to the open-loop proper frequency ω_{ol} and ξ is chosen such that it gives a good experimental results). Initial conditions are $s(0) = 0.025\ m$, $\dot{s}(0) = 0$, and $\ddot{s}(0) = 0$. The convergence time is stated as $t_F = 0.35\ s$. $\mathcal{T}$ and F defined as follows [9]:
$\mathcal{T} = [1\ 1\ 1\ 1\ 1\ 1]^T$, $\quad F = diag[-1\ -1.1\ -1.2\ -1.3\ -1.4\ -1.5\ -1.6]$.

Discontinuous Control Law: The suitable discontinuous control law is [9]: $w = -\alpha\ sgn(S)$, with $\alpha = 1.2\ 10^5$ for the electro-pneumatic actuator under interest.

The control law was implemented on the rapid prototyping board (Model 626-Sensoray), a small chattering was observed. The chattering must be eliminated by smoothing out the control discontinuity in a boundary layer $\emptyset$ neighboring the sliding surface. For the electro-pneumatic actuator under interest, the minimum suitable boundary layer was found to be $\emptyset = 200\ [m/s^2]$. Thus, the discontinuous control law becomes as $w = -\alpha\ sat(s/\emptyset) = -1.2\ 10^5\ sat(S/200)$, and the control law is defined as:

$$u = \Gamma_{nom}^{-1}\left(-X_{nom} - 1.2\ 10^5\ sat(S/200)\right) \quad (26)$$

The block diagram of the closed loop with (TOSM) controller is shown in figure (22). The real step responses of the closed loop in case of no load and maximum load are shown in figure (23). The real frequency responses of the closed loop with

various amplitudes in case of no load and maximum load are shown in figures (24) and (25), respectively.
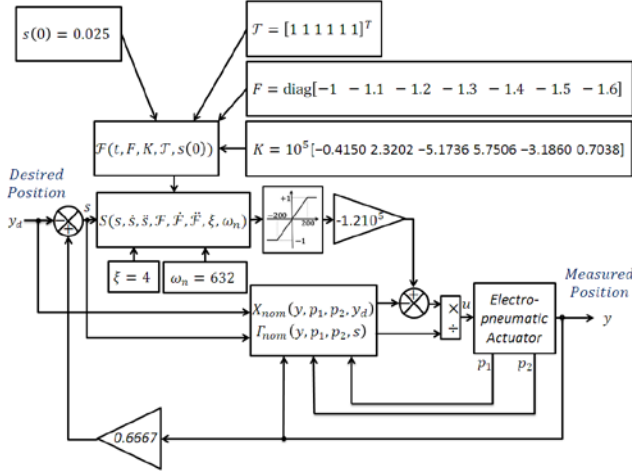
Fig. 22- The block diagram of the closed loop with (TOSM) controller.
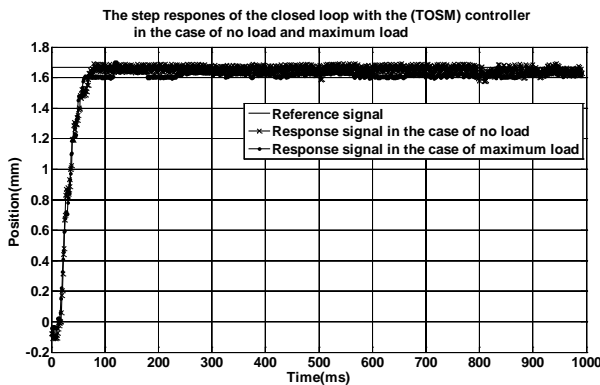
Fig. 23- The step response of the closed loop with (TOSM) controller in the case of no load and maximum load.
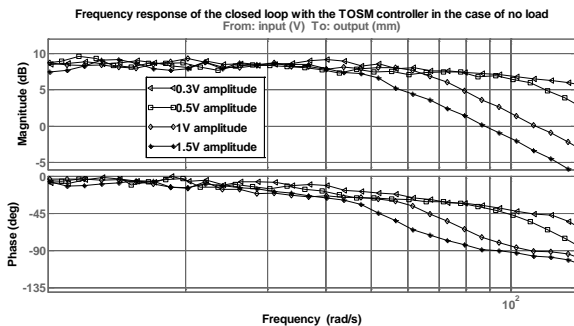
Fig. 24- The frequency response of the closed loop with (TOSM) controller in the case of no load.
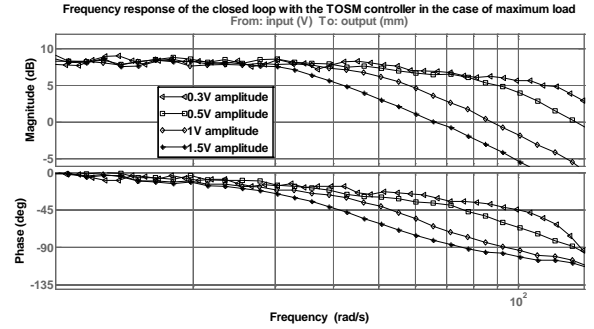
Fig. 25- The frequency response of the closed loop with (TOSM) controller in the case of maximum load.

6 The Hybrid Control Laws

6.1 The Theoretical Principle of the Hybrid Control

Let the SISO nonlinear uncertain system is defined as follows:

$$\dot{x} = f(x) + g(x)u \qquad (27)$$

Where x is the state vector, u the control input, and f, g are bounded uncertain smooth nonlinear functions. The control problem is to get the state x to track a desired state x_d.

Let the positive definite Lyapunov function $V(s) = \frac{1}{2}s^2$, where s is defined as sliding variable.

Suppose $u_{Linear}(x)$ is a linear control law that achieves the possible desired behaviour like stability and tracking accuracy for the system (27). Let the linear control law u_{Linear} converge to zero, so, it realizes the following property:

$$\begin{cases} If \ u_{Linear} > 0 \quad then \ \dot{u}_{Linear} < 0 \\ If \ u_{Linear} < 0 \quad then \ \dot{u}_{Linear} > 0 \end{cases} \qquad (28)$$

This property is always satisfied by the state feedback (PVA) and proportional-derivative (PD) control laws which will be used later in this paper.

If the sliding variable s is chosen such as $s(x) = u_{Linear}(x)$, then from (28): the equation $s\,\dot{s} < 0$ is achieved. Thus, the derivative of Lyapunov function $\dot{V}(s) = s\,\dot{s}$ is negative definite, so:

$$\exists \eta > 0: \quad \dot{V}(s) = s\,\dot{s} \leq -\eta|s| \qquad (29)$$

Obtaining the inequality in (29) means that the system is asymptotically stable and controlled in such a way that the system states always move

towards the sliding surface s and hits it in finite time [16]. As a result, the linear control law can be chosen as a sliding variable which is the idea of hybrid linear-sliding mode control.

6.2 The Hybrid GSPVA-FOSMC Controller (GSPVAFOSMC)

The hybrid GSPVA-FOSMC controller is implemented by taking the Gain-scheduled-proportional-velocity-acceleration (GSPVA) control law as a sliding variable for the first order sliding mode (FOSMC) controller.

In the context of first order sliding mode control, the gain-scheduled-proportional-velocity-acceleration (GSPVA) control law in (6) is chosen as sliding variable as follows:

$$s = K_p(y_d - y) - K_v \dot{y} - K_a \ddot{y} \qquad (30)$$

From (1) and (2), its relative degree with respect to u is equal to one. Thus, it serves as sliding variable for first order sliding mode controller: $u = -K \, sign(s)$, where $K = 1.5$.

The control law was implemented on the rapid prototyping board (Model 626-Sensoray), a small chattering was observed. The chattering must be eliminated by smoothing out the control discontinuity in a boundary layer $\emptyset$ neighboring the sliding surface. For the electro-pneumatic actuator under interest, the minimum suitable boundary layer was found to be $\emptyset = 1.25 \, [m/s^2]$, and the hybrid control law (GSPVAFOSMC) is given as follows:

$$u = -1.5 \, sat(s/\emptyset) = -1.5 \, sat\big((K_p(y_d - y) - K_v \dot{y} - K_a \ddot{y})/1.25\big) \qquad (31)$$

The block diagram of the closed loop with (GSPVAFOSMC) controller is shown in figure (26). The real step responses of the closed loop in case of no load and maximum load are shown in figure (27). The real frequency responses of the closed loop with various amplitudes in case of no load and maximum load are shown in figures (28) and (29), respectively.
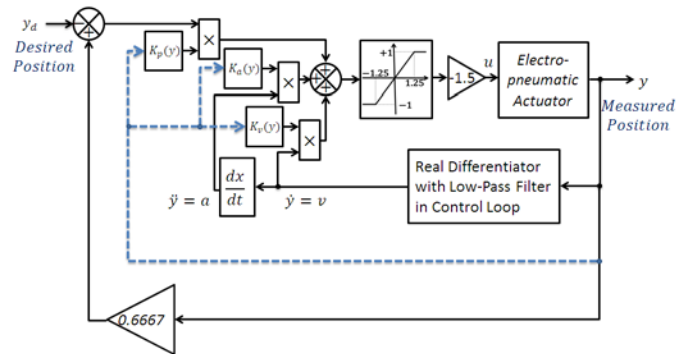
Fig. 26- The block diagram of the closed loop with (GSPVAFOSMC) controller.
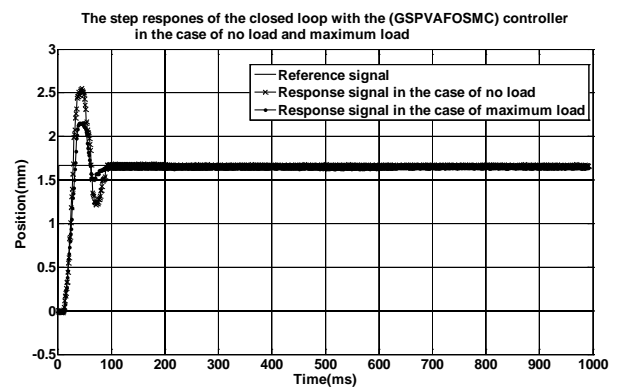
Fig. 27- The step response of the closed loop with (GSPVAFOSMC) controller in the case of no load and maximum load.
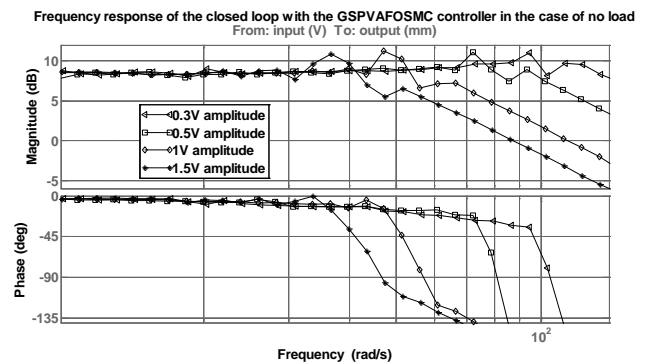
Fig. 28- The frequency response of the closed loop with (GSPVAFOSMC) controller in the case of no load.
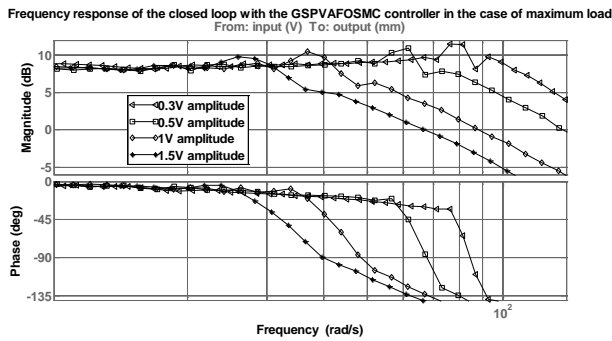
Fig. 29- The frequency response of the closed loop with (GSPVAFOSMC) controller in the case of maximum load.
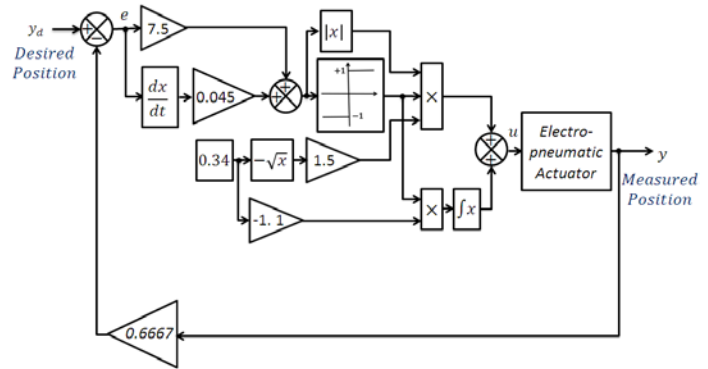
Fig. 30- The block diagram of the closed loop with (PDSTA) controller.

6.3 The Hybrid PD-STA Controller (PDSTA)

The hybrid PD-STA controller is implemented by taking the proportional-derivative (PD) control law as a sliding variable for super twist algorithm (STA) controller.

In the context of second order sliding mode control, the proportional derivative (PD) control law which is given by (10) is chosen as sliding variable.

$$s = 7.5\,e + 0.045\,\dot{e} \qquad (32)$$

Where $e = y_d - y$. From (1) and (2), its relative degree with respect to u equal to two. Thus, it serves as sliding variable for super twist algorithm (STA) which is one of second order sliding mode control method. The control law of (STA) is given as in (22) and its parameters are calculated in the same way explained in section 5.2 ($\lambda = 1.5\sqrt{C}$, $w = 1.1C$).

The control law was implemented on the rapid prototyping board (Model 626-Sensoray). The constant C has been chosen small in the beginning, then it has been increased enough to achieve good performance. The appropriate values of C was $C = 0.34\ [V/s]$.

The block diagram of the closed loop with (PDSTA) controller is shown in figure (30). The real step responses of the closed loop in case of no load and maximum load are shown in figure (31). The real frequency responses of the closed loop with various amplitudes in case of no load and maximum load are shown in figures (32) and (33), respectively.
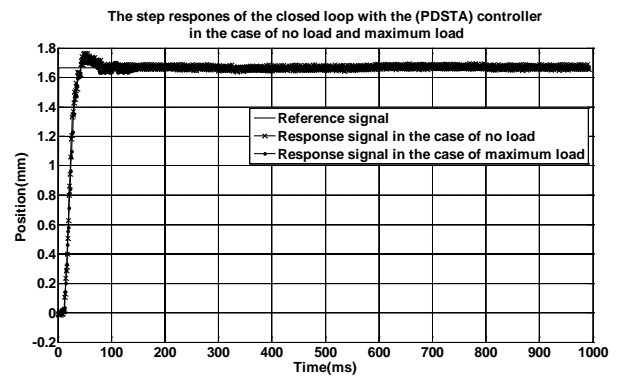
Fig. 31- The step response of the closed loop with (PDSTA) controller in the case of no load and maximum load.
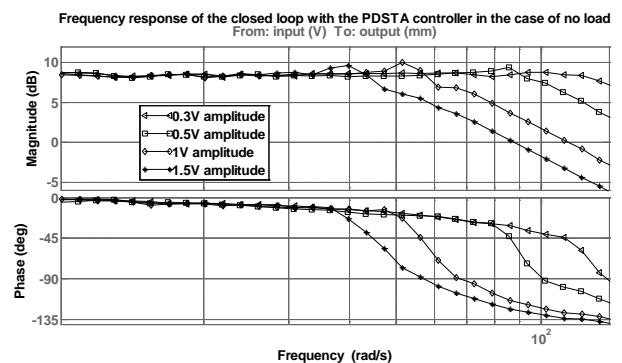
Fig. 32- The frequency response of the closed loop with (PDSTA) controller in the case of no load.
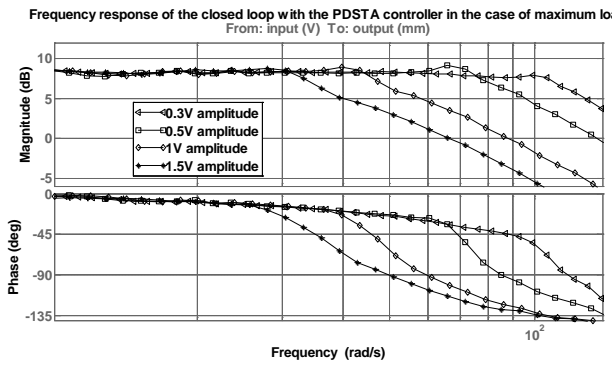
Fig. 33- The frequency response of the closed loop with (PDSTA) controller in the case of maximum load.

7 Results Analysis

The boundary layer $\emptyset$ in the classical (FOSMC) and hybrid (GSPVAFOSMC) controllers is shown in Table 1. The upper bound of disturbance dynamics C in the classical (STA) and hybrid (PDSTA) controllers is shown in Table 2.

Table 1- The boundary layer $\emptyset$ in the classical and hybrid controllers.

Controller	FOSMC	GSPVAFOSMC
$\emptyset$ [m/s^2]	400	1.25

Table 2- The upper bound of disturbance dynamics C in the classical and hybrid controllers.

Controller	STA	PDSTA
C [V/s]	0.003	0.34

The step response characteristics of the electro-pneumatic actuator in the closed-loop system for each controller are shown in Table 3 for the case of no load, and in Table 4 for the case of maximum load. Where $\overline{y}$ is the average position, $\overline{\varepsilon}$ is the average static error, σ is the standard deviation of the position, t_r is the rise time, t_s is the 5% settling time, v_{max} is the maximum velocity, and a_{max} is the maximum acceleration. In each step response, the statistics: $\overline{y}$, $\overline{\varepsilon}$, and σ were calculated from position data for 900 point of time after the settling time.

In the frequency domain, the critical parameter is the cutoff frequency (bandwidth), that is the frequency at which system's power decays to half (-3dB) the nominal pass band value. The previous definition of the cutoff frequency is related to the magnitude response only.

Table 3- The step response characteristics of the closed-loop for all the controllers in the case of no load.

Controller	GSPVA	PD	FOSMC	STA	TOSM	GSPVAFOSMC	PDSTA
$\overline{y}$ [%]	99.62	99.19	99.62	99.14	99.37	99.75	100.05
$\lvert\overline{\varepsilon}\rvert$ [%]	0.38	0.81	0.38	0.86	0.63	0.25	0.05
σ [%]	0.41	0.68	0.53	0.69	1.3	0.55	0.73
t_r [ms]	13.96	13.42	13.09	14.44	37.59	13.72	18.47
t_s [ms]	84.09	51.67	82.28	60.36	69.41	88.52	56.1
$\lvert v_{max}\rvert$ [$m.s^{-1}$]	0.14	0.129	0.142	0.125	0.0998	0.154	0.11
$\lvert a_{max}\rvert$ [$m.s^{-2}$]	14.38	14.51	13.82	12.82	12.91	12.96	11.12

Table 4- The step response characteristics of the closed-loop for all the controllers in the case of maximum load.

Controller	GSPVA	PD	FOSMC	STA	TOSM	GSPVAFOSMC	PDSTA
$\overline{y}$ [%]	97.57	98.91	97.65	98.77	97.22	98.13	99.96
$\lvert\overline{\varepsilon}\rvert$ [%]	2.43	1.09	2.35	1.23	2.78	1.87	0.04
σ [%]	0.29	0.32	0.47	0.35	0. 87	0.29	0.42
t_r [ms]	16	15.55	16	24	39	16	21
t_s [ms]	86.03	50.02	78.16	42.4	59.25	76.43	36.38
$\lvert v_{max}\rvert$ [$m.s^{-1}$]	0.101	0.0992	0.102	0.096	0.074	0.1045	0.085
$\lvert a_{max}\rvert$ [$m.s^{-2}$]	12.15	12.07	13.26	11.33	8.27	12.83	11.05

The phase shift in the phase response is very important too. So, a new definition of cutoff frequency is taken into account for the control system in this paper as follows: cutoff frequency is the frequency where the phase shift is 45° in the phase response, at the same time, the magnitude response mustn't be less than 3dB below the nominal pass band value. Thus, the cutoff frequency of the closed-loop according to the new definition is shown in Table 5 for the case of no load, and in Table 6 for the case of maximum load.

Table 5- The cutoff frequency of the closed-loop at phase shift 45° for all the controllers at various input amplitudes in the case of no load.

Test amplitude [V]	Cutoff frequency at phase shift 45° [Hz]						
	GSPVA	PD	FOSMC	STA	TOSM	GSPVAFOSMC	PDSTA
0.3	15	17.3	15	17.4	17.5	15.4	17.9
0.5	12	12.6	11.81	13	15.6	12.15	13.8
1	8.2	9	8.1	9	10.6	8.2	9.1
1.5	6.5	7	6.5	7	8.3	6.6	7.1

Table 6- The cutoff frequency of the closed-loop at phase shift 45° for all the controllers at various input amplitudes in the case of maximum load.

Test amplitude [V]	Cutoff frequency at phase shift 45° [Hz]						
	GSPVA	PD	FOSMC	STA	TOSM	GSPVAFOSMC	PDSTA
0.3	12.3	13.8	12.4	14.4	15.9	12.5	14.5
0.5	9.7	10.5	9.7	10.7	12.1	9.8	11
1	6.6	7.1	6.6	7.2	8.5	6.6	7.3
1.5	5.1	5.6	5.1	5.6	6.6	5.2	5.6

From all experimental results in the tables (1) to (6), the following points can be deduced:

- *In the case of the hybrid (GSPVAFOSMC) controller:*

-The boundary layer ($\emptyset = 1.25 \ [m/s^2]$) required for smoothing out the control discontinuity of the controller (GSPVAFOSMC) is thinner than the boundary layer ($\emptyset = 400 \ [m/s^2]$) necessary for the controller (FOSMC); this means that the controller (GSPVAFOSMC) is more robust than the controller (FOSMC).

-The controller (GSPVAFOSMC) improves the position accuracy in the case of no load (99.75%) and maximum load (98.13%) better than both controllers: (GSPVA) and (FOSMC).

-The controller (GSPVAFOSMC) improves the settling time (76.43 $[ms]$) in the case of maximum load better than both controllers: (GSPVA) and (FOSMC).

-The controller (GSPVAFOSMC) improves the closed-loop bandwidth in the cases of no load (15.4 $[Hz]$ and 12.15 $[Hz]$) and maximum load (12.5 [Hz] and 9.82 [Hz]) for small amplitudes (0.3 [V] and 0.5 [V]), respectively, better than both controllers: (GSPVA) and (FOSMC).

- *In the case of the hybrid (PDSTA) controller:*

-The upper bound of disturbance dynamics ($C = 0.34 \ [V/s]$) for the controller (PDSTA) is bigger than ($C = 0.003 \ [V/s]$) for the controller (STA), this means that the controller (PDSTA) can resist higher level of disturbance dynamics. In other words the controller (PDSTA) is more robust than the controller (STA).

-The controller (PDSTA) improves the position accuracy in the case of no load (100.05%) and maximum load (99.96%) better than both controllers: (PD) and (STA) and all other controllers.

-The controller (PDSTA) improves the settling time (36.38 $[ms]$) in the case of maximum load better than both controllers: (PD) and (STA) and all other controllers.

-The controller (PDSTA) improves the closed-loop bandwidth of the closed-loop in the cases of no load (17.9 $[Hz]$ and 13.8 $[Hz]$) and maximum load (14.5 $[Hz]$ and 11 $[Hz]$) for small amplitudes (0.3 [V] and 0.5 [V]), respectively, better than both controllers: (PD) and (STA).

-The implementation of this controller is simple and needs one feedback sensor (position sensor).

- *In the case of the (TOSM) controller:*

-The bandwidth with the (TOSM) controller is better than all other controllers for all input amplitudes in the case of no load and maximum load.

-The position accuracy in the case of maximum load is relatively worse (97.22%).

-The implementation of this controller is more complex than the other controllers and needs three feedback sensors (position sensor and two pressure sensor).

It is noted that the (TOSM) controller Achieve better bandwidth compared to other controllers. The (PDSTA) controller realizes better position accuracy and better settling time in the case of maximum load compared to other controllers, besides the good bandwidth.

Finally, the Table 7 allows the user to choose the control law that best meets his specifications. The number of signs + in the table indicates the degree of satisfaction.

Table 7- Comparative study of different control strategies.

Controller	GSPVA	PD	FOSMC	STA	TOSM	GSPVAFOSMC	PDSTA
Accuracy	++	+++	++	+++	++	+++	+++++
Time response	++	+++	++	++++	+++	++	+++++
Bandwidth	++	+++	++	++++	+++++	++	++++
Simplicity to synthesize	++	++++	++	+++	+	++	+++
Number of sensors	1	1	1	1	3	1	1
Robustness	++	+++	++	++++	+++	+++	+++++

8 Conclusion

Linear, sliding mode and hybrid controllers for an electro-pneumatic actuator system have been implemented successfully. Firstly, the linear and nonlinear models of the electro-pneumatic actuator have been presented. Thereafter, the specifications of the electro-pneumatic system under interest have been detailed. After that, the linear controllers: gain-scheduled proportional velocity acceleration (GSPVA) and the proportional-derivative (PD) have been designed and implemented. Then, the first order sliding mode controller (FOSMC), the second order sliding mode controller represented by supper twist algorithm (STA) and the third order sliding mode controller (TOSM) has been designed and implemented. Thereafter, the hybrid controllers: (GSPVAFOSMC) and (PDSTA) have been implemented after clarifying their theoretical principle. Finally, the results have been analyzed.

The results have proven that the hybrid controllers are more robust than the classical first and second order sliding mode controllers. Further, the hybrid controllers improve time and frequency domain characteristics of the closed-loop. From one hand, they improve the position accuracy in the cases of no load and maximum load; also they

improve the settling time in the cases of maximum load. On other hand, they improve the bandwidth of the closed-loop in the case of no load and maximum load. Also the results have proven that the third order sliding mode controller (TOSM) realizes better bandwidth for the closed loop. Finally, the hybrid controller (PDSTA) realizes better position accuracy, settling time, bandwidth, complexity and ease of implementation, for the electro-pneumatic actuator under interest.

References:
[1] VADIM, I. UTKIN. "Survey paper variable structure systems with sliding modes." IEEE Transactions on Automatic control 22.2 (1977).

[2] de Souza, Oldineia Batista, et al. "Adaptive Control Applied To Two Links Of A Cartesian Electropneumatic Manipulator Robot Of Three Degrees Of Freedom." ABCM Symposium Series in Mechatronics. Vol. 5. 2012.

[3] Abry, Frederic, et al. "Non-linear position control of a pneumatic actuator with closed-loop stiffness and damping tuning." European Control Conference (ECC). 2013.

[4] Riachy, Samer, and Malek Ghanes. "A nonlinear controller for pneumatic servo systems: Design and experimental tests." *Mechatronics, IEEE/ASME Transactions on* 19.4 (2014): 1363-1373.

[5] Brun, Xavier. *Commandes linéaires et non linéaires en électropneumatique. méthodologies et Applications*. Diss. 1999.

[6] Laghrouche, S., et al. "Robust second order sliding mode controller for electropneumatic actuator." *American Control Conference*. Vol. 6. 2004.

[7] Dridi, Mehdi. *Dérivation numérique: synthèse, application et intégration*. Diss. Ecole Centrale de Lyon, 2011.

[8] Girin, Alexis. *Contribution à la commande non linéaire d'un système électropneumatique pour une utilisation Aéronautique: Application sur un Benchmark dédié*. Diss. Ecole Centrale de Nantes (ECN), 2007.

[9] Girin, Alexis, et al. "High-order sliding-mode controllers of an electropneumatic actuator: Application to an aeronautic benchmark." *Control Systems Technology, IEEE Transactions on* 17.3 (2009): 633-645.

[10] Le, Minh-Quyen. Development of bilateral control for pneumatic actuated teleoperation system. Diss. INSA de Lyon, 2011.

[11] Milosavljević, Čedomir, Branislava Peruničić, and Boban Veselić."A New Real Differentiator with Low-Pass Filter in Control Loop." *FACULTY OF ELECTRICAL ENGINEERING UNIVERSITY OF BANJA LUKA*: 27.

[12] Ogata, Katsuhiko. *Modern control engineering, third edition*. Upper Saddle River, NJ: Prentice-hall, 1997.

[13] Slotine, Jean-Jacques E., and Weiping Li. *Applied nonlinear control*. Vol. 199.No. 1. Englewood Cliffs, NJ: Prentice-hall, 1991.

[14] Huangfu, Yi-Geng. *Research of Nonlinear System High Order Sliding Mode Control and its Applications for PMSM*. Diss. North Western Polytechnical University (Chine), 2010.

[15] Shtessel, Yuri, et al. "Introduction: Intuitive Theory of Sliding Mode Control." *Sliding Mode Control and Observation*. Springer New York, 2014.1-42.

[16] Bregeault, Vincent. *Quelques contributions à la théorie de la commande par modes glissants*. Diss. Ecole Centrale de Nantes (ECN), 2010.